

Article

Investigation of High Voltage Anodic Plasma (HVAP) Ag-DLC Coatings on Ti50Zr with Different Ag Amounts

Andrei Bogdan Stoian¹, Cristina Surdu-Bob², Alexandru Anghel², Daniela Ionita¹ and Ioana Demetrescu^{1,3,*}

¹ Department of General Chemistry, Faculty of Applied Chemistry and Materials Science, University Politehnica of Bucharest, 1-7 Gheorghe Polizu str., 011061 Bucharest, Romania; andreibstoian@yahoo.com (A.B.S.); daniela.ionita@upb.ro (D.I.)

² Low Temperature Plasma Laboratory, National Institute for Lasers, Plasma and Radiation Physics, 409 Atomistilor str., 077125 Magurele, Romania; cristina.surdubob@plasmacoatings.ro (C.S.-B.); alexandru.anghel@inflpr.ro (A.A.)

³ Academy of Romanian Scientists, 54 Spaiul Independentei, 050094 Bucharest, Romania

* Correspondence: ioana_demetrescu@yahoo.com; Tel.: +40-21-402-3930

Received: 18 October 2019; Accepted: 22 November 2019; Published: 26 November 2019



Abstract: The paper presents the investigation of a series of silver-incorporated diamond-like carbon (Ag-DLC) coatings with increasing Ag content on Ti50Zr and deposited using high voltage anodic plasma (HVAP). The coatings surface properties were analyzed with scanning electron microscope (SEM), atomic force microscope (AFM), and contact angle determinations. Electrochemical tests were performed in Afnor artificial saliva and evaluated by potentiodynamic polarization and electrochemical impedance spectroscopy. Based on these properties, comparisons of coatings performance were linked with the amount of deposited Ag. Increasing the Ag content led to the increase of the corrosion resistance and to the decrease of the forces exhibited on the surface. The hydrophobic character of the coating with the highest Ag amount could prevent thrombosis, thus suggesting its possible use for medical implants.

Keywords: TiZr; DLC coating; high voltage anodic plasma; surface properties; electrochemical characterization

1. Introduction

Due to its biocompatibility and corrosion resistance, titanium (Ti) is known as the gold reference for implants in dentistry [1]. Like zirconium (Zr), it is a valve metal, and its surface can form spontaneously, under normal atmospheric conditions, a thin, passive, protective oxide layer named zirconia (ZrO₂) [2]. Zr and its alloys are materials that present good mechanical strength while keeping the low toxicity of the base metal [3–5].

Alloying is a way to enlarge Zr fields of application, improving the material's properties such as resistance to corrosion, mechanical behavior, and antibacterial activity. TiZr alloys are now being investigated for implant applications due to the exceptional biocompatibility of both Ti and Zr combined with their better mechanical properties compared to pure Zr. The present manuscript's aim is to enhance properties of this alloy using an Ag-DLC coating known from previous works as antibacterial and protective in bioliquids and to test the electrochemical stability and hydrophilic character of coated surface [6,7].

Zr and Ti belong to the same group of metals, which makes them perfect candidates for co-alloying. Ti is a dimorphic metal with two phases (α and β). The binary phase diagram of Ti and Zr presents

a continuous solid solution. The fusion temperature of the Ti (1670 °C) is lowered by increasing the amount of Zr (~1640 and 1560 °C for 10 wt.% and 40 wt.% Zr) [4]. The binary alloy TiZr presents two different crystal structures— α and β . Different concentrations of Ti in the TiZr alloy have been investigated [8,9], but the one that seems to possess remarkable mechanical properties is the one containing equal amounts of the two metals [10]. The microstructure of the binary alloy Ti50Zr, changes from phase β to phase α [11], affecting the structure of the alloy and its properties. The β to α phase transformation temperature of Ti50Zr alloy is down to 630 °C. Its electrochemical stability, even in very aggressive media such as saliva [12], is remarkable, while its biocompatibility is also increased. Therefore, Zr and Zr alloys are recommended as viable alternatives to Ti for oral implants and restorative works in dentistry [13]. Moreover, the surface of TiZr can change from “bioinert” to “bioactive”, inducing multifunctional favorable biologic and mechanical peri-implant tissue responses [14]. Current studies on TiZr show that surface modifications can embed diverse molecules to mimic bone tissue structures or to affect bacterial activity [15]. In this idea, surface vitro ceramic coatings on TiZr obtained by laser ablation [16] and diamond-like carbon (DLC) films [17] were investigated for their performance in biomedical applications. Incorporation of metallic elements such as Ag [17] and Zn [18] into diamond-like carbon (DLC) films was a strategy of adding functional features regarding mechanical and antibacterial properties recommended for wear, tribology, and bioapplications. Nevertheless, future studies are required to evaluate success rates of coated TiZr implant.

Ag-DLC coatings are known for their tribological properties, which are strongly dependent on Ag quantity. Incorporating between 4.3% and 10.6% Ag into DLC coatings, a decrease of wear rate and friction coefficient simultaneous with the increase of Ag content was observed [19]. It was reported that Ag segregates from carbon due to its low solubility with carbon [20,21]. This can increase silver content at the film surface. The Ag content influence on the Ag-DLC films properties has rarely been studied and was focused on antibacterial Ag activity and biointerphase [22]. As a part of the novelty of the present manuscript, we propose to study the change of Ag-DLC film properties with increasing Ag amount, on the TiZr substrate, which is in extended use in dentistry, with the aim of identifying their suitability for implants in oral cavity applications after enhancing their properties. Thus, properties such as corrosion resistance and hydrophilic/hydrophobic character were envisaged.

As far as we know, our present work represents the first attempt to deposit and investigate Ag-DLC layers on Ti50Zr substrate and varying the Ag amount.

2. Materials and Methods

2.1. Thin Film Deposition

The films presented in this work were deposited using an original plasma source, the high voltage anodic plasma (HVAP). The main characteristic of these plasmas is the use of energetic electrons to evaporate and create a plasma plume containing atoms and ions of the anode material in high vacuum. HVAP adds a new capability, namely deposition of alloys with controlled composition by igniting a single plasma plume above the anode. HVAP is a line of sight deposition method, drawback that can be overcome by rotations and translations of the specimen in order to be deposited evenly.

The experimental setup is presented elsewhere [23,24] and therefore only a brief description is given here. An anode containing the material to be deposited is bombarded with energetic electrons of several hundred eV. The material is thus evaporated and a plasma is ignited by collision of electrons with vapors. In this work, 25 mm diameter Ag-C anodes with increasing Ag content were used. The amount of Ag introduced in each C anode used for the five deposition experiments undertaken in this work is presented in Table 1. Ag concentrations ranging from 0 to 8.3 and this selection were in accord with literature research for Ag amount in Ag-DLC study of mechanical properties [25]. Typical deposition parameters were 3.3 A discharge current, 440 V discharge voltage, deposition time 5 min, 30 cm anode-substrate distance. Deposition rate decreased with increasing Ag/C ratio from 2.4, 0.15, to 0.13 nm/s, respectively. The resulted film's thickness varies between 39 and 720 nm. The substrates

were optical grade polished Ti50Zr alloy disks of 2.5 cm diameter. Before deposition, the samples were cleaned by ultrasonication 15 min in acetone and 15 min in isopropyl alcohol.

Table 1. Amount of Ag introduced in each C anode.

Sample	A1	A2	A3	A4
Ag in anode (%)	0	1.8	5.6	8.3
Deposition rate nm·s ⁻¹	1.33	2.4	0.15	0.13

2.2. Surface Analysis

The micro surface morphologies and compositions of the Ti50Zr samples coated and non coated with Ag-DLC were investigated with a Quanta 650 scanning electron microscope (SEM) from FEI (Hillsboro, OR, USA) equipped with an energy dispersive X-ray analysis (EDX) module in high vacuum at 10 kV. Atomic force microscopy (AFM) investigations, including morphology, surface roughness and force-distance adhesion curves, were performed in contact mode with a A100-SGS system from APE Research (Trieste, Italy). To evaluate the hydrophilic-hydrophobic character, contact angles were measured and are reported as the average of 10 measurements of a 3 µL droplet using KSV Instruments (Helsinki, Finland) CAM 100 equipment.

2.3. Electrochemical Stability

The electrochemical tests were performed in Afnor artificial saliva with a composition (g/L) of NaCl 0.7; KCl 1.2; Na₂HPO₄ 0.26; NaHCO₃ 1.5; KSCN 0.33; CH₄ON₂ 1.35 [25] using an Autolab PGSTAT 302N (Metrohm AG, Herisau, Switzerland) in a system with a conventional three electrode cell with the Ti50Zr sample as the working electrode, a Pt foil as the counter electrode, and a Ag/AgCl the reference electrode. Before each measurement, the potential was left to stabilize for 10 min at open circuit. The electrochemical impedance spectroscopy (EIS) measurements were performed at frequencies between 10 kHz and 0.1 Hz, with a signal amplitude of 10 mV vs. open circuit potential (OCP). Polarization data were registered between ±200 mV and OCP using a scan rate of 0.2 mV/s and represented as Tafel plots. Electrochemical data were evaluated and fitted using Nova 1.10 software.

3. Results and Discussion

3.1. Surface Characterization

Figure 1a shows the surface of the polished Ti50Zr substrate covered in native oxide formed naturally in atmosphere. SEM images of all coated samples (Figure 1b–e) show that the HVAP coating process covered the surface of the substrate with a DLC film. According to literature data in Ag-DLC coatings, Ag particles are dispersed in the amorphous carbon matrix [26] and, depending on the Ag amount, a process of surface segregation of silver may take place in time. As can be seen in Figure 1c–e, Ag nanoparticles and clusters (200–400 nm) are present on the surface of samples A2, A3, and A4. This observation is sustained more clearly with AFM research. Silver segregation from the carbon matrix to film surface is also confirmed by data in the literature data [20].

AFM studies were carried out to further investigate the hybrid film morphology and are given in Figure 2. As can be observed in Figure 2a, the Ti50Zr substrate is covered in irregular native oxide that give the surface a relatively high roughness. Sample A1 (Figure 2b) is very smooth, the irregularities of the Ti and Zr oxide being covered by the DLC film. Samples A2 and A3 (Figure 2c,d) have visible Ag nanoparticles scattered on the surface. In the case of sample A4 (Figure 2e), the film with the highest Ag content, a number of silver clusters are present on the surface formed by aggregation. The aspect ratio between the diameter and height of clusters suggested that surface clusters were not spherical but rather grew in a more oblate shape. Formation of clusters can be primarily attributed to the low affinity of silver with the carbon within the matrix and the high cohesive energy of silver [27]. The roughness

of the samples slightly increased with the Ag content of the coating due to the existence of the Ag nanoclusters on the surface of the samples.

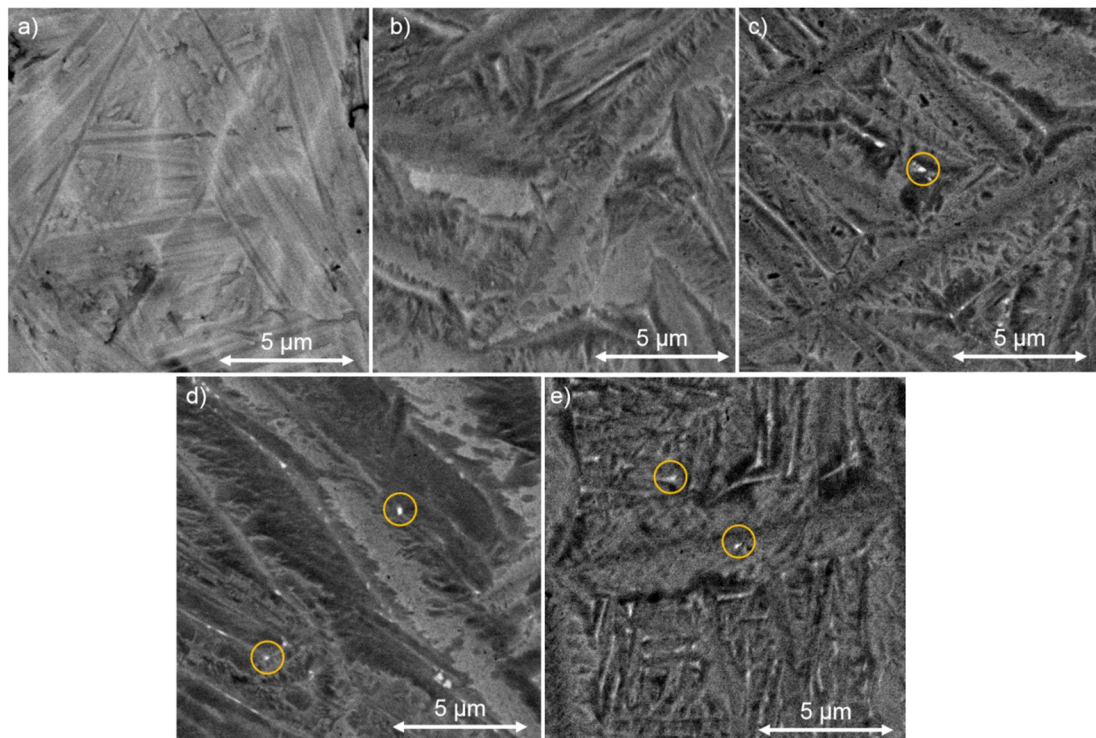


Figure 1. Micrographies for (a) Ti50Zr polished substrate and samples coated with Ag-DLC (b) A1; (c) A2; (d) A3; (e) A4. Ag clusters marked on images.

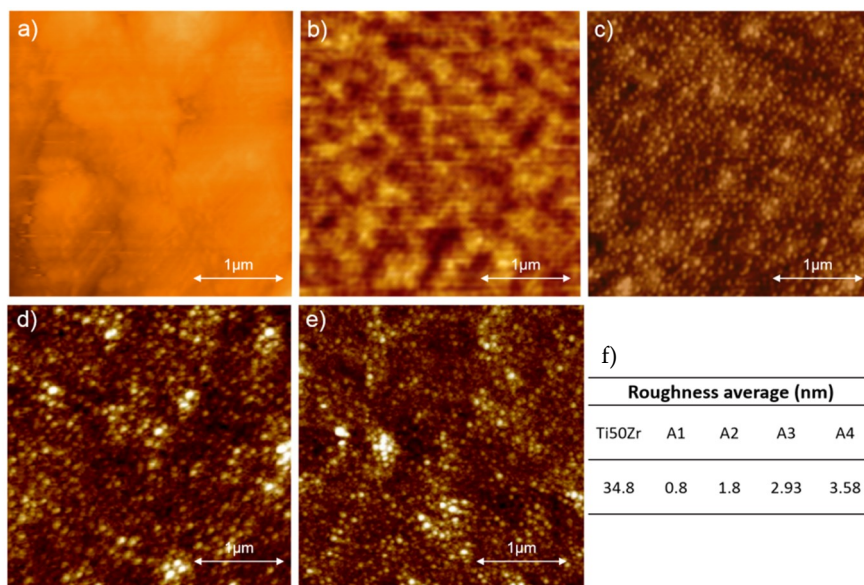


Figure 2. Atomic force microscopy (AFM) micrographies for (a) Ti50Zr polished substrate and samples coated with Ag-DLC (b) A1; (c) A2; (d) A3; (e) A4. (f) The average roughness values of the samples.

3.2. Film Composition

EDX data (Figure 3) permitted the determination of Ag quantity deposited in the films and show the increase of the Ag signal with the increase of the Ag content of the Ag-C anode used in the

fabrication of the samples. The peaks corresponding to each element were fitted to the base of the peak, thus countering the effects of different intensities registered for Ti and Zr.

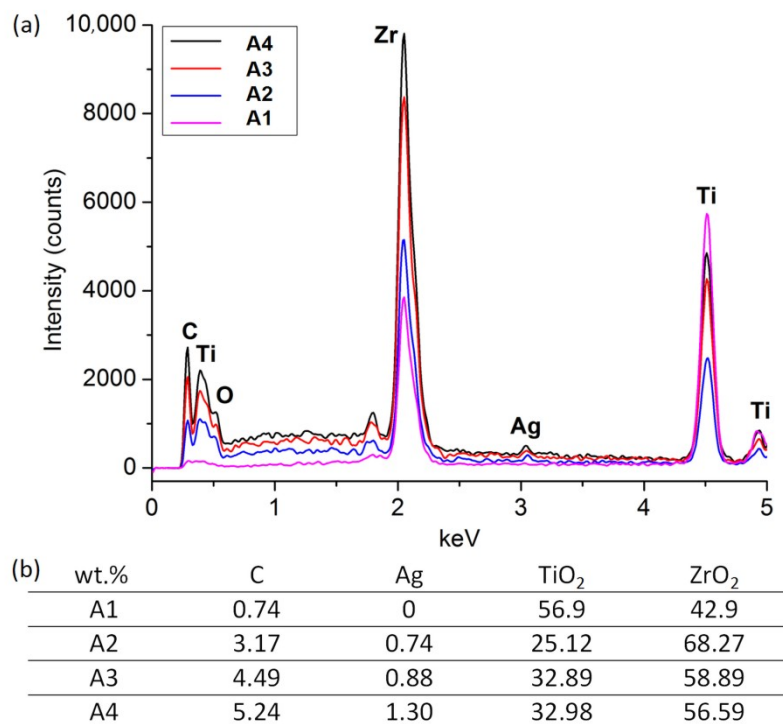


Figure 3. Recorded (a) energy dispersive X-ray analysis (EDX) signals for coated samples and (b) calculated values for elements.

The contact angle determinations (Figure 4) showed that the Ti50Zr substrate has a highly hydrophilic character. The coating with the DLC raised the contact angle value with about 50°. It appears that even the small quantities of Ag in the film have a great impact on the contact angle values since there is a transition from hydrophilic to hydrophobic from pure DLC coated sample to the sample containing the greatest amount of Ag.

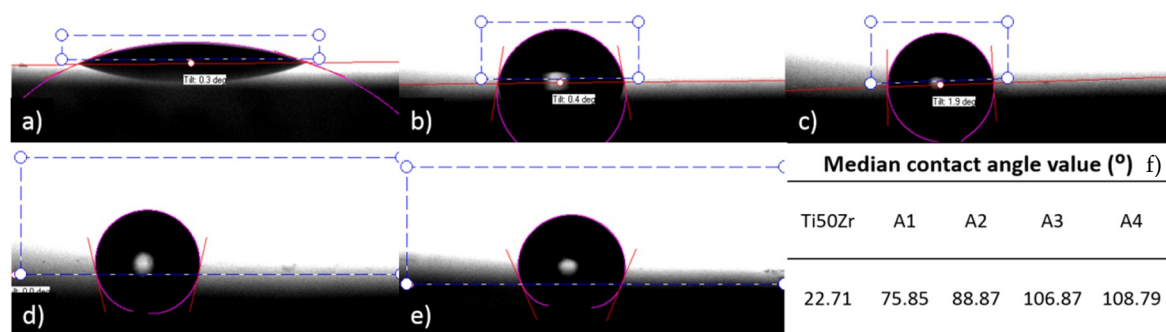


Figure 4. Representative contact angle images for (a) Ti50Zr polished substrate and samples coated with Ag-DLC (b) A1; (c) A2; (d) A3; (e) A4. (f) The median values representing the average of five measurements.

The F-Z curves measured by AFM (Figure 5) show that adhesion forces of surfaces are directly dependent on the Ag content of the sample. The trend is a decrease of surface forces with the increase of Ag content. Measured forces range between 42 nN for the sample covered only with DLC and 2 nN on the sample with the highest Ag content. Adhesive forces measured by AFM in air are generally regarded to be dominated by non-surface-specific capillary forces. However, surface roughness and

surface electrostatic forces should not be ignored. The addition of Ag increased both the roughness and the contact angle value of the sample. The adhesion force depends strongly on whether the substrate is hydrophilic or hydrophobic.

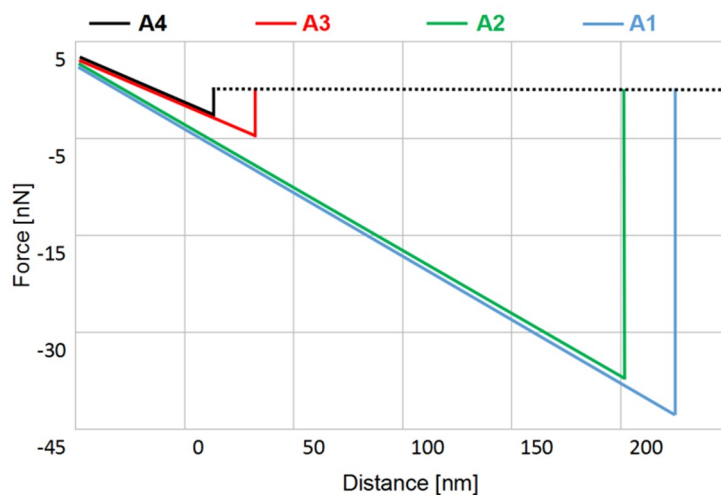


Figure 5. Normalized F-Z curves for coated samples.

3.3. Electrochemical Characterization

The stability and corrosion of samples were studied with electrochemical impedance spectroscopy (EIS) in the form of Nyquist and Bode plots and Tafel plots, respectively [28,29].

According to the Bode plots (Figure 6a), in the low frequency range between 0.01 and 100 Hz the phase angle around -79° for A3, -76° for A4, and -68° for A2 and A1, respectively, remained nearly constant. In the high frequency range (1–10 kHz) the phase angle of all samples varied rapidly between -5° and -35° .

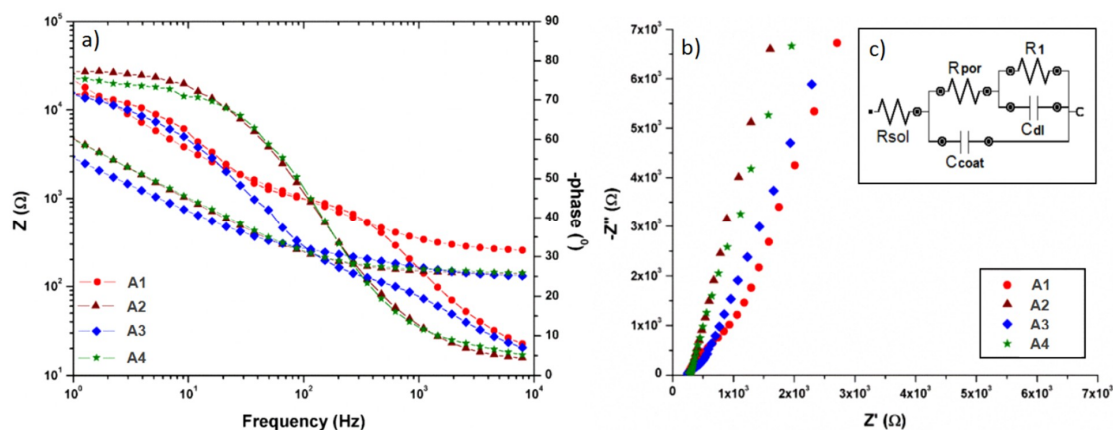


Figure 6. Electrochemical impedance spectroscopy (EIS) representations as a function of Ag amount in coatings. (a) Bode plots; (b) Nyquist plots; (c) equivalent circuit.

From the Nyquist plots (Figure 6b), it is evident that the diameters of the semicircle for the coated samples increased with the increase of the Ag/C ratio. The equivalent circuit (Figure 6c) was developed by the process of data fitting of the recording EIS spectra. The electrochemical equivalent circuit model consists of resistance and constant phase elements (CPE). The CPE is used to change in the relaxation times as a result of different degrees of surface non homogeneity. The impedance with the capacitance can be defined as $Z_{CPE} = [Q(j\omega^n)]^{-1}$, where Q , j , ω and n are the pseudo-capacitance or non-ideal capacitance. When $n = 1$ the system behaves like a pure capacitor [30]. In our case the

equivalent circuit consists of the following elements; R_{sol} is the the solution resistance of the electrolyte, and C_{coat} is the capacitance of the coating including pores in the outer layer coating; R_{por} is the pore resistance resulting from the formation of ionic conduction paths across the coating (higher R_{por} values indicate a lower pores size); C_{dl} is the double layer capacitance of the coating; R_1 is the charge transfer resistance of the coating/substrate interface. Table 2 shows the EIS parameters obtained after fitting the equivalent circuits.

Table 2. Parameters for fitted EIS circuits.

Sample	R_{sol} [$\Omega \cdot cm^2$]	R_{por} [$K\Omega \cdot cm^2$]	C_{coat} [$\mu F \cdot cm^2$]	n_1	R_1 [$K\Omega \cdot cm^2$]	C_{dl} [$\mu F \cdot cm^2$]	n_2
A1	266	106.2	6.48	0.792	277.0	22.62	0.861
A2	262	204.9	3.86	0.854	616.51	18.6	0.823
A3	252	305.6	2.01	0.898	968.25	10.24	0.712
A4	258	386.8	1.62	0.878	1098.12	8.32	0.789

Figure 7 shows the potentiodynamic polarization curves obtained for coated TiZr samples in Afnor artificial saliva. Using Stern-Geary equation the corrosion current was determined [29]. Table 3 gives the values of electrochemical parameters for all coated samples.

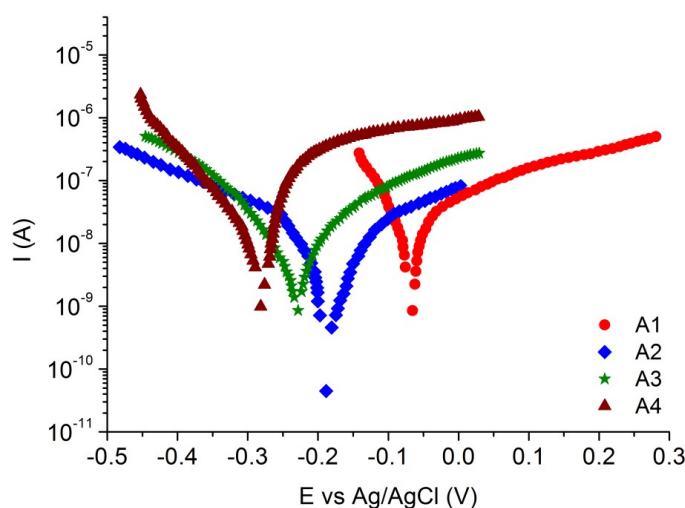


Figure 7. Tafel plots of Ag-DLC coatings with various Ag content.

Table 3. Electrochemical parameters from Tafel plots.

Sample	I_{corr} ($nA \cdot cm^{-2}$)	E_{corr} (V)	V_{corr} ($\mu m \cdot year^{-1}$)	R_p ($MOhm \cdot cm$)
A1	47.11	-67.40	4.94	1.813
A2	37.02	-274.47	4.73	3.32
A3	6.26	-157.39	1.89	5.233
A4	4.26	-193.43	1.87	5.614

According to Table 3, the Ag-DLC coating exhibits a lower corrosion current (I_{corr}) compared with DLC without Ag. The corrosion resistance (V_{corr}) is increased by the Ag amount in the coating. The results indicate that the Ag-DLC coatings improve the corrosion resistance of Ti50Zr sustaining in such way the electrochemical data from Tafel procedure. The polarization resistance (R_p) increases with the increase of the Ag content from the coating. The more evident electronegative value for corrosion potential (E_{corr}) corresponds to highest Ag amount as well.

Based on experimental data interesting correlations between contact angle, roughness, adhesion force, corrosion rate, and Ag amount were established (Figure 8). The samples' roughness, contact angle, and corrosion resistance increased with the Ag amount in the coating, with the contact angles reaching hydrophobic values. An inverse relationship was found between the Ag content in the film and the force-distance profiles of the surfaces. Comparing the corrosion rate of the Ag-DLC coating on TiZr with the one obtained in previous works [6,7] on other implant materials (such as Ti- and CoCr-based alloys, respectively), we have observed that the trend is the same and the Ag-DLC coatings decrease the corrosion representing a promising protection. It should be noted that it is not a comparison in the same conditions for both deposition and electrolyte testing. In the previous paper about Ti coated with the same film [7], the increase of Ag is connected to more hydrophilic coating, and such a fact is supposed to be in the favor of a better cell response [31,32].

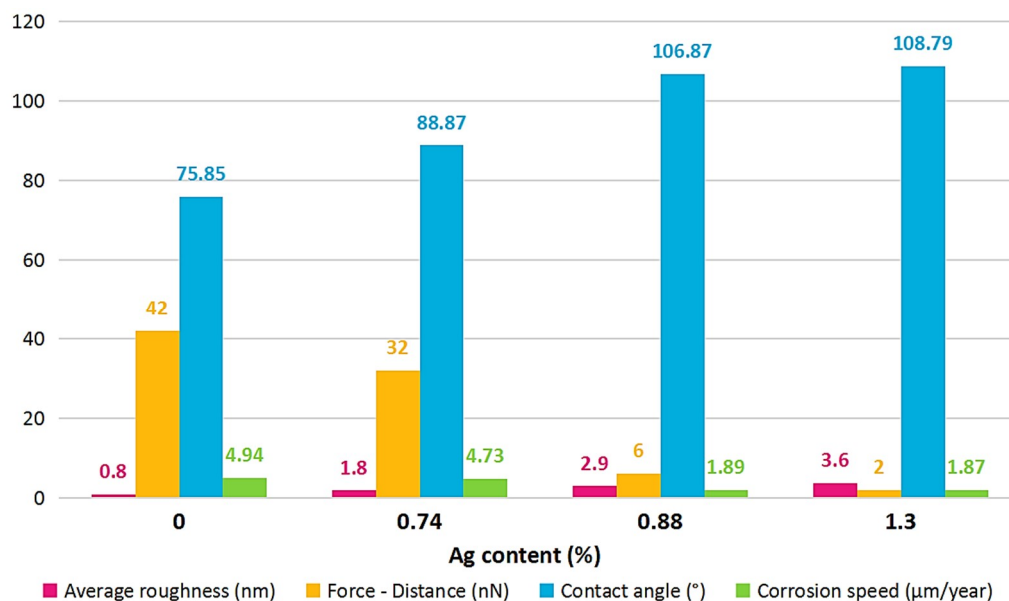


Figure 8. Correlation of sample properties and Ag content.

4. Conclusions

The paper presents an investigation of the properties of Ag-DLC coatings with different Ag content deposited using high voltage anodic plasma. Based on the characterization of the samples, we can conclude that high voltage anodic plasma (HVAP) is a versatile and powerful tool able to control the composition of thin coatings and thus affecting their properties to a degree suited to the desired applications. Based on the studied properties, we can fix a limit for the Ag amount in the films based on the fact that its increase could affect the cell response.

Author Contributions: Conceptualization, I.D., D.I. and C.S.-B.; Methodology, I.D., D.I. and C.S.-B.; Validation, I.D. and C.S.-B.; Formal Analysis, A.B.S., A.A. and D.I.; Investigation, A.B.S., A.A. and D.I.; Data Curation, A.B.S., I.D., D.I. and C.S.-B.; Writing—Original Draft Preparation, A.B.S., I.D., D.I. and C.S.-B.; Writing—Review and Editing, A.B.S. and I.D.; Visualization, A.B.S.; Supervision, I.D. and C.S.-B.; Project Administration, I.D.; Funding Acquisition, I.D.

Funding: This work was supported by the Romanian Government National Council of Scientific Research in Higher Education (CNCSIS)—Executive Unit for Financing Higher Education, Research, Development and Innovation (UEFISCDI), project numbers PN-III-P4-ID, PCE 2016-0316, and PN 19150101.

Acknowledgments: The SEM analyses on Quanta 650 FEG were possible due to European Regional Development Fund through Competitiveness Operational Program 2014-2020, Priority axis 1, Project No. P_36_611, MySMIS code 107066, Innovative Technologies for Materials Quality Assurance in Health, Energy and Environmental—Center for Innovative Manufacturing Solutions of Smart Biomaterials and Biomedical Surfaces (INOVABIOMED).

Conflicts of Interest: The authors declare no conflict of interest.

References

1. Darvell, B.W. *Materials Science for Dentistry*, 9th ed.; Woodhead Publishing: Cambridge, UK, 2009.
2. Ionita, D.; Grecu, M.; Ungureanu, C.; Demetrescu, I. Modifying the TiAlZr biomaterial surface with coating, for a better anticorrosive and antibacterial performance. *Appl. Surf. Sci.* **2011**, *257*, 9164–9168. [[CrossRef](#)]
3. Bernhard, N.; Berner, S.; De Wild, M.; Wieland, M. The binary (TiZr) alloy—A newly developed (Ti) alloy for use in dental implant. *Forum Implant.* **2009**, *5*, 30–39.
4. Liu, X.; Chen, S.; Tsoi, J.K.H.; Matinlinna, J.P. Binary titanium alloys as dental implant materials—A review. *Regen. Biomater.* **2017**, *4*, 315–323. [[CrossRef](#)] [[PubMed](#)]
5. Gradin, H.M.; Berner, S.; Dard, M. A review of titanium zirconium (TiZr) alloys for use in endosseous dental implants. *Materials* **2012**, *5*, 1348–1360. [[CrossRef](#)]
6. Ionita, D.; Golgovici, F.; Mazare, A.; Badulescu, M.; Demetrescu, I.; Pandealea-Dobrovicescu, G.-R. Corrosion and antibacterial characterization of Ag-DLC coating on a new CoCrNbMoZr dental alloy. *Mater. Corros.* **2018**, *69*, 1403–1411. [[CrossRef](#)]
7. Mazare, A.; Anghel, A.; Surdu-Bob, C.; Totea, G.; Demetrescu, I.; Ionita, D. Silver doped diamond-like carbon antibacterial and corrosion resistance coatings on titanium. *Thin Solid Film.* **2018**, *657*, 16–23. [[CrossRef](#)]
8. Izquierdo, J.; Bolat, G.; Mareci, D.; Munteanu, C.; González, S.; Souto, R. Electrochemical behaviour of ZrTi alloys in artificial physiological solution simulating in vitro inflammatory conditions. *Appl. Surf. Sci.* **2014**, *313*, 259–266. [[CrossRef](#)]
9. Akimoto, T.; Ueno, T.; Tsutsumi, Y.; Doi, H.; Hanawa, T.; Wakabayashi, N. Evaluation of corrosion resistance of implant-use Ti–Zr binary alloys with a range of compositions. *J. Biomed. Mater. Res. B Appl. Biomater.* **2018**, *106*, 73–79. [[CrossRef](#)]
10. Zhou, Y.K.; Jing, R.; Ma, M.Z.; Liu, R.P. Tensile strength of (Zr-Ti) binary alloy. *Chin. Phys. Lett.* **2013**, *30*, 116201. [[CrossRef](#)]
11. Cui, W.; Liu, Y. Fatigue behavior of Ti50Zr alloy for dental implant application. *J. Alloys Compd.* **2019**, *793*, 212–219. [[CrossRef](#)]
12. Romonti, D.E.; Gomez Sanchez, A.V.; Milošev, I.; Demetrescu, I.; Ceré, S. Effect of anodization on the surface characteristics and electrochemical behaviour of Zr in artificial saliva. *Mater. Sci. Eng. C* **2016**, *62*, 458–466. [[CrossRef](#)]
13. Sivaraman, K.; Chopra, A.; Narayan, A.I.; Balakrishnan, D. Is zirconia a viable alternative to titanium for oral implant? A critical review. *J. Prosthodont. Res.* **2018**, *62*, 121–133. [[CrossRef](#)]
14. Schünemann, F.H.; Galárraga-Vinueza, M.E.; Magini, R.; Fredel, M.; Silva, F.; Souza, J.C.M.; Zhang, Y.; Henriques, B. Zirconia surface modifications for implant dentistry. *Mater. Sci. Eng. C* **2019**, *98*, 1294–1305. [[CrossRef](#)] [[PubMed](#)]
15. Ionita, D.; Vardaki, M.; Stan, M.S.; Dinischiotu, A.; Demetrescu, I. Enhance stability and in vitro cell response to a bioinspired coating on zirconium alloy with increasing chitosan content. *J. Bionic Eng.* **2017**, *14*, 459–467. [[CrossRef](#)]
16. Busuioc, C.; Voicu, G.; Zuzu, I.D.; Miu, D.; Sima, S.; Iordache, F.; Jinga, S.I. Vitroceramic coatings deposited by laser ablation on Ti–Zr substrates for implantable medical applications with improved biocompatibility. *Ceram. Int.* **2017**, *43*, 5498–5504. [[CrossRef](#)]
17. Písařík, P.; Jelínek, M.; Remsa, J.; Mikšovský, J.; Zemek, J.; Jurek, K.; Kubinová, Š.; Lukeš, J.; Šepitka, J. Antibacterial, mechanical and surface properties of Ag-DLC films prepared by dual PLD for medical applications. *Mater. Sci. Eng. C* **2017**, *77*, 955–962. [[CrossRef](#)]
18. Hatada, R.; Flege, S.; Rimmler, B.; Dietz, C.; Ensinger, W.; Baba, K. Surface structuring of diamond-like carbon films by chemical etching of zinc inclusions. *Coatings* **2019**, *9*, 125. [[CrossRef](#)]
19. Manninen, N.K.; Ribeiro, F.; Escudeiro, A.; Polcar, T.; Carvalho, S.; Cavaleiro, A. Influence of Ag content on mechanical and tribological behavior of DLC coatings. *Surf. Coat. Technol.* **2013**, *232*, 440–446. [[CrossRef](#)]
20. Wang, L.J.; Zhang, F.; Fong, A.; Lai, K.M.; Shum, P.W.; Zhou, Z.F.; Gao, Z.F.; Fu, T. Effects of silver segregation on sputter deposited antibacterial silver-containing diamond-like carbon films. *Thin Solid Film.* **2018**, *650*, 58–64. [[CrossRef](#)]
21. Cloutier, M.; Turgeon, S.; Busby, Y.; Tatoulian, M.; Pireaux, J.J.; Mantovani, D. Controlled distribution and clustering of silver in Ag-DLC nanocomposite coatings using a hybrid plasma approach. *ACS Appl. Mater. Interfaces* **2016**, *8*, 21020–21027. [[CrossRef](#)]

22. Cloutier, M.; RTolouei, R.; OLesage, O.; Lévesque, L.; Turgeon, S.; Tatoulian, M.; Mantovani, D. On the long term antibacterial features of silver-doped diamond like carbon coatings deposited via a hybrid plasma process. *Biointerphases* **2014**, *9*, 029013. [[CrossRef](#)] [[PubMed](#)]
23. Surdu-Bob, C.; Mustata, I.; Iacob, C. General characteristics of the Thermoionic Vacuum Arc plasma. *J. Optoelectron. Adv. Mater.* **2007**, *9*, 2932–2934.
24. Surdu-Bob, C.; Vladoiu, R.; Badulescu, M.; Musa, G. Control over the sp^2/sp^3 ratio by tuning plasma parameters of the thermoionic vacuum arc. *Diam. Relat. Mater.* **2008**, *17*, 1625–1628. [[CrossRef](#)]
25. Choi, H.W.; Choi, J.H.; Lee, K.R.; Ahn, J.P.; Oh, K.H. Structure and mechanical properties of Ag-incorporated DLC films prepared by a hybrid ion beam deposition system. *Thin Solid Film.* **2007**, *516*, 248–251. [[CrossRef](#)]
26. Manninen, N.; Escobar Galindo, R.; Carvalho, S.; Cavaleiro, A. Silver surface segregation in Ag-DLC nanocomposite coatings. *Surf. Coat. Technol.* **2014**, *267*, 90–97. [[CrossRef](#)]
27. Chakravadhanula, V.S.; Kübel, C.; Hrkac, T.; Zaporojtchenko, V.; Strunskus, T.; Faupel, F.; Kienle, L. Surface segregation in TiO_2 -based nanocomposite thin films. *Nanotechnology* **2012**, *23*, 495701. [[CrossRef](#)]
28. Li, D.; Lin, C.; Batchelor-McAuley, C.; Chen, L.; Compton, R.G. Tafel analysis in practice. *J. Electroanal. Chem.* **2018**, *826*, 117–124. [[CrossRef](#)]
29. Popa, M.V.; Demetrescu, I.; Vasilescu EIonita, D.; Vasilescu, C. Stability of some dental materials in oral biofluids. *Rev. Roum. Chim.* **2005**, *50*, 399–406.
30. Milošev, I.; Kosec, T.; Strehblow, H.H. XPS and EIS study of passive film formed on orthopaedic Ti–6Al–7Nb alloy in Hank’s physiological solution. *Electrochim. Acta* **2008**, *53*, b3547–b3558. [[CrossRef](#)]
31. Demetrescu, I.; Pirvu, C.; Mitran, V. Effect of nano-topographical features of Ti/TiO₂ electrode surface on cell response and electrochemical stability in artificial saliva. *Bioelectrochemistry* **2010**, *79*, 122–129. [[CrossRef](#)]
32. Ponsonnet, L.; Reybier, K.; Jaffrezic, N.; Comte, V.; Lagneau, C.; Lissac, M.; Martelet, C. Relationship between surface properties (roughness, wettability) of titanium and titanium alloys and cell behavior. *Mater. Sci. Eng. C* **2003**, *23*, 551–560. [[CrossRef](#)]



© 2019 by the authors. Licensee MDPI, Basel, Switzerland. This article is an open access article distributed under the terms and conditions of the Creative Commons Attribution (CC BY) license (<http://creativecommons.org/licenses/by/4.0/>).